16èmes Journées de l'Hydrodynamique

27-29 novembre 2018 - Marseille

PREDICTION DES EFFORTS HYDRODYNAMIQUES SUR UN CABLE A PROXIMITE D'UN FOND RUGUEUX

Modification of a Wake model for hydrodynamic forces on submarine cables with a rough seabed

K.I. KUZNETSOV[(1)], J. C. HARRIS[(1)], L. AL ASMAR[(1)], N. GERMAIN[(2)], F. ARISTODEMO[(3)]

(1) LHSV, Ecole des Ponts, CEREMA, EDF R et D, Chatou, France
(2) France Energies Marines, MRE array layout and network integration
(3) Dipartimento di Ingegneria Civile, Universitá della Calabria

Résumé

Ce papier présente les développements récents de la modélisation numérique des efforts hydrodynamiques sur un câble dans les conditions hydrodynamiques extrêmes rencontrées sur les sites hydroliens. Les résultats des calculs CFD sont utilisés afin de créer une base de données permettant d'exprimer les efforts hydrodynamiques appliqués sur le câble par le moyen d'une formulation semi-empirique. Le modèle sera validé par une comparaison des efforts mesurés lors d'essais en bassin.

Summary

In the present work we consider the forces on a fixed slender cylinder, laying on the seabed or with some vertical height, in order to understand the stability of submarine cables, in particular for cases with large seabed roughness. Semi-empirical Wake models have been developed which include some physical understanding of the problem, shown to be accurate for a given range of parameters specific to the oil and gas industry, and until now have been used for bottom-attached cylinders. For the general case, unlike the case of a cylinder resting on the seabed, one must handle complex vertical forces due to vortex shedding. Once this is taken into account, we are able to reproduce the horizontal and vertical forces on a cylinder with a Wake model, even for cases when the cylinder is not resting directly on the seabed. The model will be validated by a comparison of the efforts measured during basin tests.

I – Introduction

Most industry guidelines (e.g., DNV GL) for predicting forces or the stability of a horizontal slender cylinder (i.e., pipeline or cable) are based on experience in the oil and gas industry, where currents and waves are relatively mild, and with seabeds of small roughness, as compared to new installations in the offshore renewable energy industry. In some regions like the Raz Blanchard, where the seabed is covered with boulders and is very rough, there is a strong interest in developing offshore renewable energy resources, but an important problem is connecting such an offshore installation to onshore power stations. Another effect of a rocky seabed is that many armoring systems for submarine cables are extremely expensive or impractical, and so it would be useful to know the forces on a cylinder near the seabed in such conditions.

In this paper, we consider the hydrodynamic forces on a single fixed (i.e. quasi-static) section of a cylindrical cable (Fig. 1). Physically, this involves a cylinder (diameter D) of a certain distance (e) from the seabed, with a seabed roughness k_s^{bed}, and a smooth or rough cylinder of roughness k_s^{cyl}. The flow is considered to be two-dimensional; while often currents and waves are not perpendicular to the cable, they will be in the case of maximum forces, which is most important for stability purposes.

The background flow we consider could have both waves and currents; this can be characterized by an oscillatory velocity at the seabed of U_m, a period T, and a background current velocity U_c, which we take to be the time-average velocity at 10 m off the seabed. This reference height is sufficiently large to be outside of the wave boundary layer even for very rough seabeds and large waves, and is significantly smaller than the depths in the area we will be considering, which has a typical depth of 40 m. Because physically the most difficult problem is understanding the interaction between the cylinder and the seabed, we assume that the region of interest is close enough to the seabed that we do not need to consider the vertical motion of the fluid due to the waves.

Finally, we are interested in the horizontal and vertical forces ($F_H(t)$ and $F_L(t)$, respectively) over time. (We therefore do not consider the rotational force on the cylinder.) To better understand the parameter ranges that we need to consider, we first identify typical conditions for a site of interest, described next.

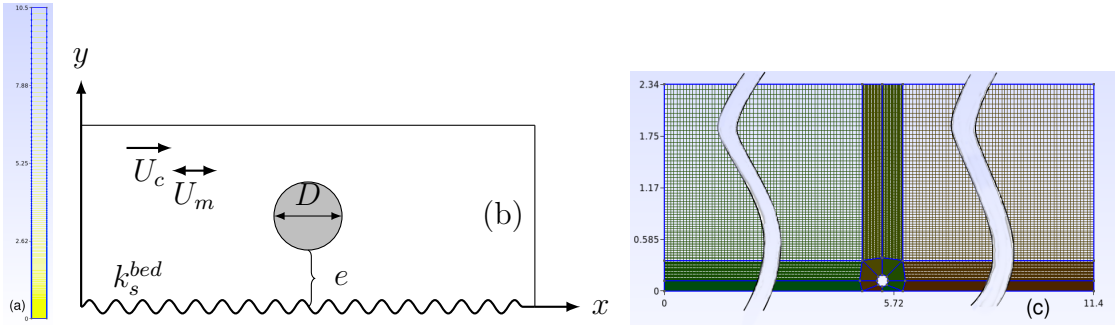

FIGURE 1 – Definition sketch, with a relative height, e/D, a Reynolds number, $Re = |U_m + U_c|D/\nu$, a current ratio, U_c/U_m, a Keulegan-Carpenter number, $KC = U_m T/D$, and a relative seabed roughness, k_s^{bed}/D, where the background flow can be taken to be $U_\infty = U_c + U_m \sin(2\pi t/T)$.

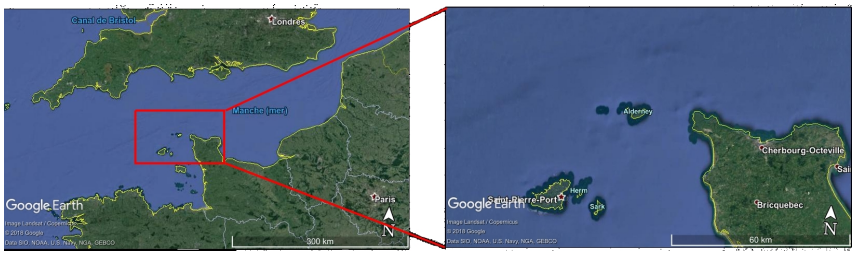

FIGURE 2 – Map of Raz Blanchard (Alderney Race), on the northern French coastline.

I – 1 Site-specific conditions

As an example of a site where one could find a rough seabed and an interest in installing submarine cables, we will consider here the Raz Blanchard (also known as the Alderney Race), which is renowned for having very strong currents and waves (Fig. 2). There are numerous studies of the conditions in the English Channel, mostly concerning the tidal current distribution, such as Coggan and Diesing [6]. Tidal current measurements from Thiebot et al. [19] show that mean current velocity in region mainly vary between 0 and 2 m/s and could be as high as 5 m/s in places. Other simulations by Coggan et al. [6] suggest that the mean value of effective roughness height in Raz-Blanchard area is k_s^{bed} is 10 cm and at some areas it could be as high as 20 cm.

As a result, we are particularly interested in understanding cases with : a seabed roughness $z_0^{bed} = k_s^{bed}/30$ between 0.1 mm and 4 cm ; an average current U_c (at reference height 10 m off the seabed) between 0 m/s and 6 m/s ; a bottom wave velocity U_w between 0.01 m/s and 2.5 m/s ; a wave period, T, between 3 s and 18 s ; and a cable (which we take to have a diameter of 13 cm) of a variety of heights.

I – 2 Existing datasets for forces on cylinders

A wide variety of tests have also looked at steady flow on a cylinder near a wall, such as Bearman and Zdravkovich [3]. Oscillatory flow on a cylinder, with the intended application of submarine pipelines, was first studied extensively by Sarpkaya [15].

Later, a wider range of experimental campaigns were undertaken by Bryndum et al. [4], who looked at forces on a cylinder lying on the seabed in a wide range of $KC = 7 - 100$ and Reynolds numbers $Re = 10^5 - 10^6$. Although roughness was considered, it was for relatively small boundary layer thicknesses. Alternatively, Sumer et al. [18] conducted experimental study of flow around a moving cylinder placed at some distance from plane boundary.

There have not been many tests for large seabed roughness, or for very large boundary layer thickness, but forces on a cylinder in the presence of background shear has been extensively studied. An early, relatively complete study of forces on cylinders in shear was conducted by Kiya [9] who performed wide range of laboratory tests and analytical studies of turbulent flow past cylinder laying on different distances from seabed.

More recently, Oner et al. [12] presented a laboratory study of interaction of a current with a circular cylinder near a rigid bed. The resulting velocity profiles, streamlines and isovorticity contours are presented for a variety of gap ratios, e/D. Experiments indicate that the changes in the flow structure become very slow when $e/D \geq 0.3$, and the wall proximity effect on the flow around the cylinder becomes insignificant when $e/D \geq 1.0$.

Increasingly there is more numerical work considering these types of flows ; Sarkar and

Sarkar [14] ran large-eddy simulations of the wake dynamics and turbulence characteristics behind a circular cylinder placed near a wall for varying gap-to-diameter (e/D) ratios.

I – 3 Various simplified models of forces on cylinders

We begin with a background velocity field $U_\infty(t)$, ignoring the structure of the boundary layer at the moment,

$$U_\infty(t) = U_c + U_m \sin(\omega t) \tag{1}$$

where we have a sinusoidal component and some background current, though this can be extended to irregular or nonlinear waves (notably in works of Aristodemo et al. [2]).

In the simplest case and most classical approach, one could use Morison's equation [20] for the calculations of the horizontal and vertical forces for a cable near the seabed. Unfortunately, the Morison approach does not describe the force time-series well, particularly for the vertical force ; see e.g., see Bryndum et al. [4].

A more comprehensive approach is to decompose the force measurements of experimental data into a variety of Fourier coefficients ; this approach is well developed by Bryndum et al. [5], and used by the Pipeline Research Council International (PRCI). By capturing the Fourier coefficients of the resulting forces for every condition required, one can predict easily the time-series of force on the cylinder, but this requires a large database of results, and does not provide much physical insight into the resulting flow.

Starting with the Exxon Pipeline Field Measurement Program described by Lambrakos et al. [10], semi-empirical Wake models have been developed which take into account the changes in the background flow due to the presence of the cylinder. This original Wake I model was later updated by Soedigdo et al. [17], improved to consider waves with currents by Sabag et al. [13], and recently tested for random waves with a simplified derivation of the velocity field in the wake of a cylinder by Aristodemo et al. [2]. In a Wake model, it is noted that the cylinder does not interact with the background flow directly, but an effective velocity, u_e :

$$u_e(t) = U_\infty(t) + u_w(t) \tag{2}$$

where $U_\infty(t)$ is the background flow, and $u_w(t)$ is the effect of the wake. Instead of constant coefficients, as in the Morison approach, one has,

$$F_H(t) = \frac{1}{2}\rho D C_D(t)|u_e(t)|u_e(t) + \frac{\pi}{4}\rho D^2\left(C_M\frac{dU_\infty(t)}{dt} + C_{AW}\frac{du_w(t)}{dt}\right), \tag{3}$$

$$F_L(t) = \frac{1}{2}\rho D C_L(t)u_e^2(t) + \frac{\pi}{4}\rho D^2\left(C_{MV}\frac{dv(t)}{dt}\right), \tag{4}$$

with time-varying drag coefficient, C_D, and lift coefficient, C_L, as well as a constant horizontal and vertical inertia coefficient, C_M and C_{MV}, and added mass coefficient associated with the wake flow passing the cylinder, C_{AW}, and free steam vertical velocity, $v(t)$. In our case free stream vertical velocity is zero.

For cylinders resting on the seabed, experiments have shown that the lift and drag coefficients can be parameterized as :

$$C(S/D) = C^{st} + \alpha(S/D)^\beta \exp\left(\gamma(S/D)^\delta\right) \tag{5}$$

where C is the lift or drag coefficient, C^{st} is the steady value, and α, β, γ, and δ are variables which vary depending on how quickly the force achieves steady-state. The variable S is the distance traveled by the cylinder versus the background flow, that is $S(t) = \int u_e(t)dt$.

The main difference between different Wake models is the development of the wake velocity, $u_w(t)$; interestingly, this approach has given good results over a wide range of parameters making use of the linearized Navier-Stokes equations for determining this velocity. Each Wake model has been shown to be accurate for a given range of parameters, but each have different limitations, such as being calibrated for a particular range of Keulegan-Carpenter number, and are calibrated only for the bottom-attached cylinders. We will consider here how these can be extended for raised cylinders.

II – Governing equations and methods

Code_Saturne is a CFD code for laminar and turbulent flows, developed at EDF R&D. Using a finite volume method, it solves the Reynolds averaged Navier–Stokes (RANS) equations :

$$\nabla \cdot \bar{u} = 0, \tag{6}$$

$$\rho \frac{\partial \bar{u}}{\partial t} + \nabla \bar{u} \cdot (\rho \bar{u}) = -\nabla \bar{p} + \nabla \cdot (\tau - \rho \mathbf{R}) + S_u, \tag{7}$$

where ρ is the fluid density, S_u is momentum source term (which can be used to impose an additional pressure gradient), τ is the viscous stress tensor, $\mathbf{R}$ is a Reynolds stress tensor. *Code_Saturne* has been implemented with a large range of first- and second-order turbulence models (see Archambeau et al. [1] for details). Two domains are used in this paper : first a one-dimensional domain (Fig. 1a) and next a two-dimensional domain (Fig. 1b and Fig. 1c). For both, the domain has only one cell thick in the z-direction.

In order to compute far-field boundary conditions, both the velocity and turbulent statistics profiles are stored ; this is done by first running a one-dimensional *Code_Saturne* test case (Fig. 1a) with periodic boundary conditions in x- and $z-$directions with pressure-gradient forcing in the form :

$$\frac{dp}{dx} = \frac{2\pi U_m}{T} \cos \frac{2\pi t}{T} + p_x^{const}, \tag{8}$$

where p_x^{const} is a constant pressure gradient related to the steady current. (This approach assumes that we do not consider the effect of the spatial variation of the wave-current interaction in this problem, which is reasonable, as the wavelength of the dominant waves are more than 100 m, for a cable of diameter 13 cm.) For cases with an oscillatory component, we impose a particular constant pressure gradient, and then determine the reference velocity from the measured velocity profiles in *Code_Saturne* .

Saving the profiles of this domain at each point in time, they are applied as far-field boundary conditions to the 2D domain shown in Fig. 1. (It is possible to use periodic boundary conditions in the x-direction, but that would require a very large domain.)

III – Simulations of flow near smooth boundary

The final application requires accurate representation of the wave-current boundary layer, the forces on time-varying flow around a cylinder, and the effect of the seabed ; in order to validate each aspect, let us start by considering cases with a smooth, flat seabed, for which there are many experimental datasets to validate the CFD results.

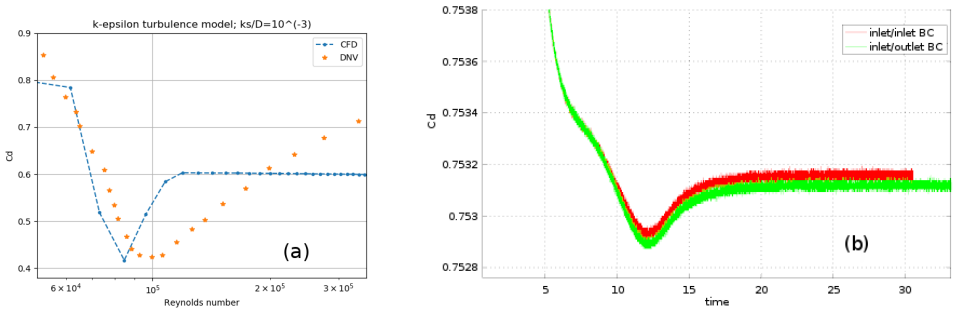

FIGURE 3 – (a) : Comparison of drag coefficients calculated by *Code_Saturne* and provided by [7] for cylinder with roughness $k_s^{cyl}/D = 10^{-3}$. (b) : Comparison of $C_D(t)$ calculated by classical inlet/outlet boundary conditions and by inlet conditions on both sides of the domain cable roughness $3.1 \cdot 10^{-5}$. The cylinder here is three diameters from the lower boundary, a symmetry (no-stress) condition ($e = 3D$).

III – 1 Steady flow : tests of boundary conditions

If we first consider steady flow, there have been many measurements of lift and drag coefficient ; a summary of many classical results can be found in the Recommended Practice DNV-RP-C205 [7]. Fig. 3a shows that results numerical simulations matches to guidelines provided by DNV-RP-C205 [7]. Here we compare steady flow around the rough cylinder which has roughness $k_s^{cyl}/D = 10^{-3}$ for Reynolds number between 0.5×10^5 and 3.5×10^5. This can further be used as an assurance that we can properly represent the critical regime of turbulent flow around the cylinder [16].

In order to simulate oscillatory flow affected to the cylinder we need to impose boundary conditions on the left and the right side of the domain. In case of combined wave-current flow we need to be sure that calculations are stable when cylinder wake will achieve the boundary. To check that, we run simulations with prescribed boundary conditions on the both sides of the domain and compare them to classical inlet/outlet boundary conditions. Fig. 3b shows a reasonable match of results so we can assume that this issue will not cause instabilities to the next calculations.

III – 2 Oscillatory flow

Alternatively, Sumer et al. [18], made measurements of forces on cylinders under oscillatory conditions, with different parameters (KC, e/D, k_s^{cyl}, Re), thus we are able to consider all aspects except for the seabed roughness and background current.

We find that *Code_Saturne* can reproduce experimental data for turbulent flow around a cylinder (for test conditions with $KC = 20$ and $e/D = 0.4$; Fig. 4), with the exception of very low KC values, which are not the primary focus of this investigation. The resulting database of hydrodynamic forces on cylinders for a wide range of conditions will be a reference for an updated Wake model adapted for our conditions, discussed below.

IV – Simulations of flow near rough boundary

IV – 1 Wave-current interaction (without cylinder)

Next, let us consider wave-current interaction close to the seabed, without any obstacles, both to verify if this corresponds to existing models such as Madsen [11], and

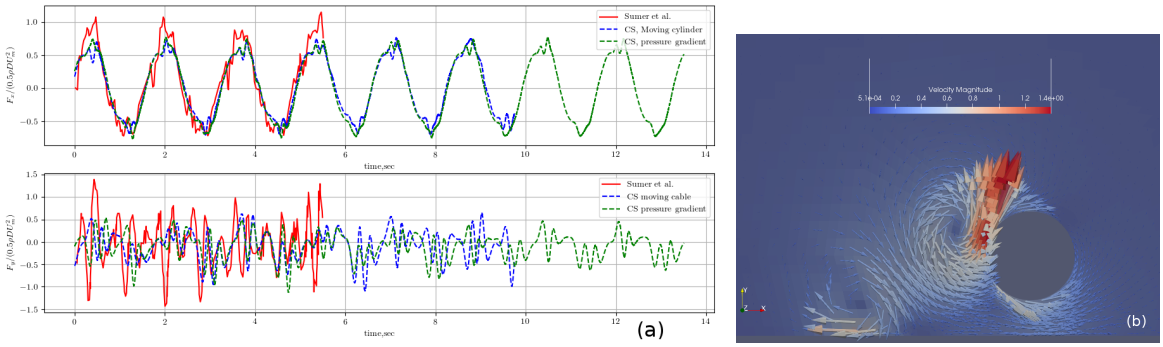

FIGURE 4 – (a) : Comparison between experimental results of [18] and *Code_Saturne* modeling results for $KC = 20$ and $e/D = 0.4$, horizontal force (upper plot), vertical force (lower plot). (b) : Velocity field behind the moving cylinder at $t = 0.1$ s.

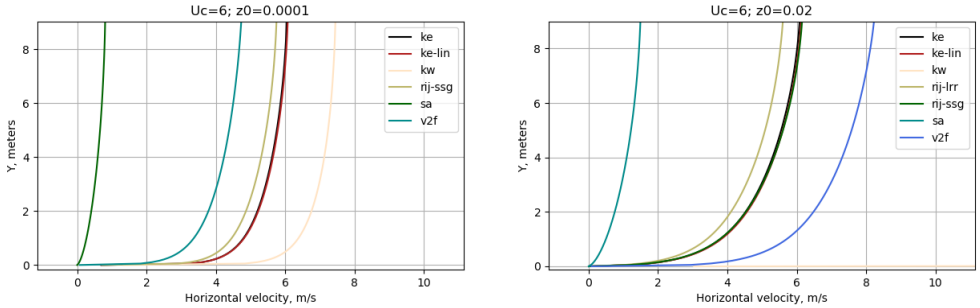

FIGURE 5 – Comparison of horizontal velocity profiles calculated over the 1-D domain using different turbulence models.

to generate boundary conditions for the next section. The approach of Madsen is based around the linearized boundary layer equation for the velocity, that is :

$$\frac{\partial u}{\partial t} = -\frac{1}{\rho}\frac{\partial p}{\partial x} + \frac{\partial}{\partial y}\left(\nu_t \frac{\partial u}{\partial y}\right) \tag{9}$$

where ν_T is the turbulent eddy viscosity, which was taken to be proportional to the height over the seabed height and either a combined wave-current shear velocity, for points within the wave boundary layer, or the current-induced shear velocity, for points outside of the wave boundary layer.

The steady flow consists of a log-layer, both outside and inside the wave boundary layer (though with different shear velocities), and the oscillatory component which corresponds to the wave boundary layer solution is equivalent to the Grant and Madsen [8] solution. As noted by Madsen, however, this type of eddy viscosity approach may have limitations when the wave boundary layer thickness is smaller than the seabed roughness k_s^{bed}, which might explain why the match with *Code_Saturne* is poor for some cases when $k_s^{bed} > 0.3$ m.

Steady flow To choose the best turbulence model for the final application, we first test different turbulence models available with *Code_Saturne* for range of needed parameters $(z0, U_c)$ and compare them to theoretical logarithm profile for a typical grid resolution. Constant pressure gradient was applied over the 1-D domain which is periodic in $x-$ and $z-$directions (Fig. 1a). The domain is quite high ($h = 10.5$ meters) to allow us to use in our database the reference height at $h_{ref} = 10.0$ meters. A vertically stretched grid is used to efficiently consider such a large domain.

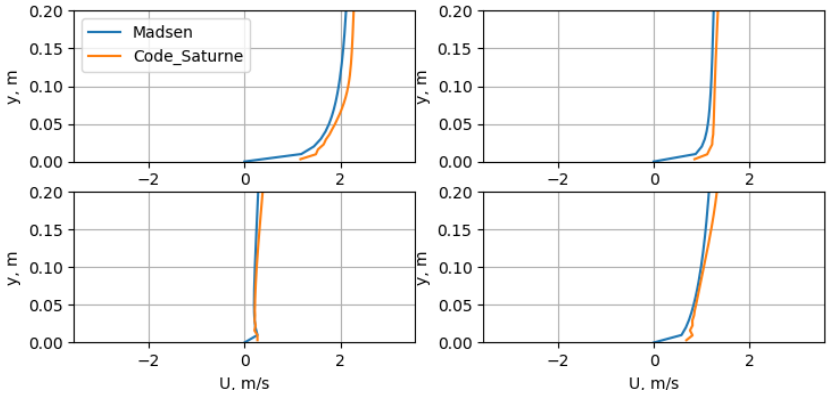

FIGURE 6 – Plot of horizontal velocity profiles at different phases calculated by *Code_Saturne* as an example of a catalogue record. This case is corresponding to (top left figure is corresponding to $\phi = \pi$, bottom left is $\phi = 0$, bottom right is $\phi = \pi/2$, top right is $\phi = 3\pi/2$)

From many RANS approaches (i.e., $k-\epsilon$, $k-\epsilon$ Linear Production, $k-\omega$ SST, Spalart-Allmaras, $R_{ij}-\epsilon$ SSG, $R_{ij}-\epsilon$ LLR, v^2-f) for the extreme conditions of seabed roughness ($k_s^{bed} = 0.003, 0.6$ m) and current velocities ($U_c = 0.1, 6.0$ m/s), as we can see from Fig. 5 the most robust models to describe developed turbulent flow over the rough seabed are $k-\epsilon$, $R_{ij}-\epsilon$ SSG and $k-\epsilon$ Linear Production models. In our next numerical simulations we will only use these turbulence models. Naturally it is likely that the other models also should reproduce the log-layer (e.g., with finer mesh resolution), but given that we need to run a great number of simulations we need to use a robust turbulence model appropriate for our simulations. Preliminary tests show that $k-\epsilon$ and $R_{ij}-\epsilon$ approaches here are relatively insensitive to grid choice.

Combined wave-current flow To compare the Madsen model [11] with these calculations, we perform 250 numerical tests with a wide range of parameters, including : a seabed roughness k_s^{bed} between 3 mm and 60 cm; an average current U_c (at reference height 10 m off the seabed) between 0.2 m/s and 6.0 m/s; a bottom wave velocity U_m between 0.1 m/s and 2.5 m/s; and a wave period, T, between 3 s and 18 s.. The vertical profiles of the results are saved each quarter-period ($T/4$), for the duration of the simulation.

We can compare the results to theoretical model of Madsen [11]. Results match well in case of small seabed roughness (Fig. 6) but less so in case of big seabed roughness (e.g., $k_s^{bed} > 0.3$ m). Results shown in Fig. 6 correspond to a case with $U_m = 0.9$ m/s, and a period $T = 13.0$ s, and a pressure gradient which induces a steady current at the reference height of 10 m of $U_c = 2.06$ m/s. This corresponds roughly in 40 m depth to waves of height $H = 5.35$ m.

IV – 2 Steady turbulent flow around a cylinder near a boundary

For our applications, we need to reproduce the flow around a cylinder, not just the wave-current background flow. If we consider steady flow, we have drag and lift coefficients which depend on the Reynolds number, gap ratio, and roughness of the seabed and cable. Fig. 7 shows that for a cylinder far from the seabed and for small seabed roughness ($k_s^{bed} = 3$ mm), one obtains a drag coefficient near 1.2, typical for this Reynolds number,

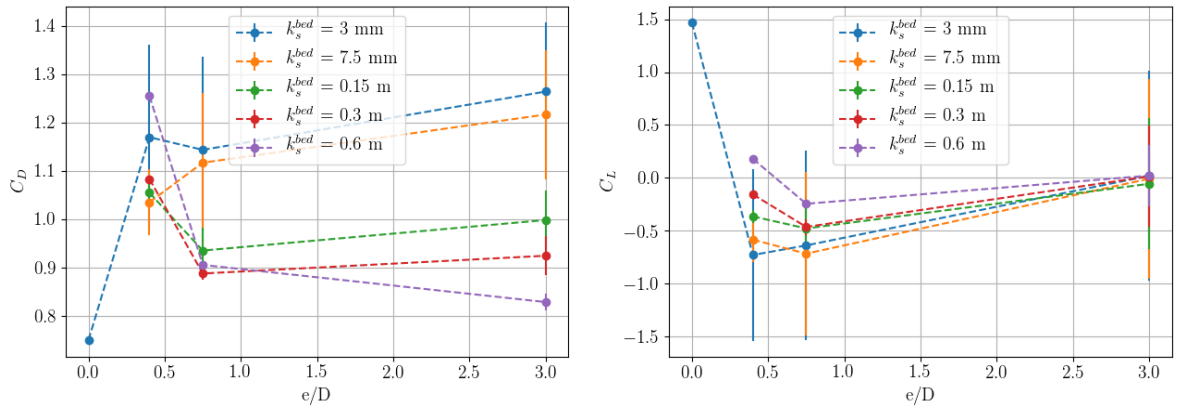

FIGURE 7 – Mean drag and lift coefficients ($C = F/(0.5\rho DU^2)$) calculated for different proximity to the rough seabed calculated for horizontal velocity $U_c = 1.67$ m/s at 10.0 m reference height and cable with small roughness $k_s^{cyl} = 0.51$ mm with $R_{ij} - \epsilon$ SSG turbulence model (vertical lines indicate standard deviation).

and an average lift coefficient near zero. Behavior of the lines is close to guidelines by DNV [7].

It also shows that as cylinder approaches the seabed, the lift coefficient increases, a well-known phenomenon. But in case cylinder is close to the seabed lift coefficient appears negative which is unusual, this could be due to the choice of turbulence model. Future updated results should explain this phenomena. Note standard deviations of the lift coefficients indicate significant vortex shedding, even for rough seabeds, for a cable height e/D of 0.4 or 0.75. Some results do not match completely existing published data for uniform flows, but here there is a large shear close to the seabed, resulting in a significant difference between the velocity at the top and bottom of the cylinder in some situations.

V – Modification of Wake models

Finally, we are interested in knowing if we can adapt a Wake II model to handle cases with an elevated cylinder, unlike earlier works by Soedigdo et al. [17], Sabag et al. [13], or Aristodemo et al. [2]. If we consider the test cases of Sumer et al. [18], we can compare the results of experiment, *Code_Saturne* , and such a modified Wake II model in a case where we do not have the complexity of the bottom boundary layer, which will be considered in future works.

To compare, Soedigdo et al. [17] used a more complex expression for the wake velocity (under the assumption that the eddy viscosity is harmonic), but constant values of coefficients such as C_M (see Eq. 3) ; this expression for the wake velocity also assumed that the flow was harmonic. Aristodemo et al. [2] produced a much simpler equation of the wake velocity (and therefore could be applied more easily to irregular or nonlinear waves), but did not need to consider the same range of KC values, and as a consequence required to adjust values of C_M, γ_L and δ_L as a function of KC number in order to match results.

Tests are ongoing comparing different types of Wake models, as ultimately we have the goal of modeling such irregular waves, but for this paper, we return to the equations of Soedigdo et al. [17] for oscillatory flow ; in this case, we need to modify the wake velocity formulation for a raised cylinder, and afterwords we need to recalibrate the start-up function for lift and drag, using *Code_Saturne* , as there is no published data for this.

V – 1 Wake velocity for raised cylinder

To summarize, in Soedigdo et al. [17], the velocity of the flow in the wake is estimated by essentially solving a linearized version of Prandtl's boundary layer equations, assuming a constant eddy viscosity in the wake. Then considering oscillatory flow only, the form of the wake velocity has a form of $U_w h(t) \exp\left(-(y/D)^2 g^2(t)\right)$, as given by Schlicting [16]. The final form of the equation is :

$$u_{w,seabed} = \int_{-D/2}^{D/2} U_m C_1 \sin^n(\omega t + \phi) \exp\left(-y^2 C_2^2 \sin^{2n}(\omega t + \phi)/D^2\right) dy. \tag{10}$$

As we are dealing with the linearized Navier-Stokes equations, we can combine multiple solutions ; notably, if the boundary layer has no effect on the drag of the cylinder, we can apply a symmetry (i.e., no-stress) condition at the seabed, and obtain a final wake velocity formula of :

$$U_w = \frac{\sqrt{\pi} U_m C_1}{2C_2} \left[\mathrm{erf}\left(C_2 \sin^n(\omega t + \phi)\right) - \mathrm{erf}\left(2C_2 \frac{e}{D} \sin^n(\omega t + \phi)\right)\right. \tag{11}$$

$$\left. + \mathrm{erf}\left(C_2 \frac{D + 2e}{D} \sin^n(\omega t + \phi)\right)\right] \tag{12}$$

In fact the starting assumption of the linearized Navier-Stokes equations is somewhat questionable, but earlier Wake models have been quite successful at determining the forces on a cylinder. The more important difference is the vertical momentum terms, but this lack is partially addressed in the start-up function, described next, and will be shown to provide a moderately reasonable agreement.

V – 2 Start-up function for raised cylinder

The force on a cylinder varies in time ; in a Wake model, this is assumed to be related to coefficients (e.g., drag, lift), which can vary in time, unlike in a Morison approach. To determine this time-dependence, one can consider an impulse test, where a cylinder initially at rest is suddenly moved at a constant velocity. In this case, the forces on the cylinder are not affected by the wake, the background flow is constant, and the coefficient can be directly related to the horizontal and vertical forces measured.

For a raised cylinder, vortex-shedding can occur which will mean that the forces may not be steady but in fact oscillatory. We therefore replace Eq. 5 with :

$$C_D(S/D) = \alpha_D (S/D - C_D^{st})^{\beta_D} \exp\left(\gamma_D (S/D)^{\delta_D}\right), \tag{13}$$

$$C_L(S/D) \text{ is defined by } \textit{Code\_Saturne} \text{ calculations for every particular case.} \tag{14}$$

where the curve fit for the coefficients in the drag start-up function are $\alpha_D = 0.55$, $\beta_D = 1.0$, $\gamma_D = -0.45$, $\delta_D = 0.82$, and the steady coefficient is $C_D^{st} = 0.5$. The lift coefficient start-up function was simply taken to be an interpolation of the measurements, due to the varying lift force, as a result of vortex shedding, causing difficulties in the choice of an appropriate analytic function.

Note that the concept behind a start-up function is based around the assumption that the seabed boundary layer does not affect the drag of the cylinder ; for applications with a rough seabed, we are looking in future work at replacing this concept with a semi-analytic solution of boundary equations which take into account the roughness of the seabed.

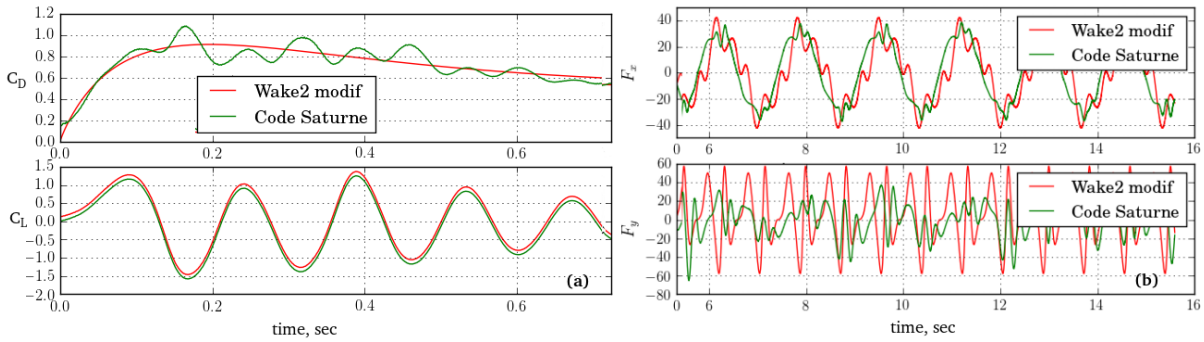

FIGURE 8 – Modified Wake II model adjusted for the case with $KC = 20$, $e/D = 0.4$ and a smooth cylinder. New start-up function for the case (left) and comparison with *Code_Saturne* calculation (right).

V – 3 Matching of results for smooth boundaries

Preliminary results show that proper choice of model parameters can reproduce forces even for complex cases (Fig. 8b) ; for this test case, *Code_Saturne* was run for the case of $KC = 20$, $e/D = 0.4$ and a smooth cylinder and seabed. The resulting force predicted by the Wake model has a variety of high-frequency components which do not appear in the *Code_Saturne* predictions, but the drag force has a relatively low error, and the maximum lift force is reproduced.

VI – Summary

This paper summarizes a work-in-progress for numerical modeling of wave-current interaction with a cylinder near to the seabed. Due to the wide range of conditions needed, this effort has required an automated system of running hundreds of test cases.

Overall, we see that traditional RANS modeling using k-ϵ or $R_{ij} - \epsilon$ models reproduces the wave-current interaction model of Madsen [11], as expected, and RANS modeling of a moving cylinder near a smooth seabed can reproduce the forces measured by Sumer et al. [18]. Further, modifications of existing Wake II models appear to be capable to handle the situation where a cylinder is not lying on the seabed, and match experiment as well.

Finally, while there exists relatively little experimental data for forces on cylinder near a very rough, rocky boundary, CFD modeling shows that there is a significant effect of the bottom boundary layer on these forces ; inclusion of this effect on the Wake model to enable a more complete understanding of submarine cable stability will be the subject of future work.

VII – Acknowledgements

We would like to thank Nicolas Relun and Christophe Peyrard for helpful discussions. This work is performed under financial support of grant ANR-10-IEED-0006-20, France Energies Marines project STHYF (STabilité de câble et HYdrodynamique de Fond).

References

[1] F. Archambeau, N. Méchitoua, and M. Sakiz. Code saturne : a finite volume method for the computation of turbulent incompressible flows - industrial applications.

International Journal on Finite Volumes, 1 :1–62, 2004.

[2] F. Aristodemo, G. R. Tomasiccho, and P. Veltri. New model to determine forces at on-bottom slender pipelines. *Coastal Engineering*, 58 :267–280, 2011.

[3] P. W. Bearman and M. M. Zdravkovich. Flow around a circular cylinder near a plane boundary. *Journal of Fluid Mechanics*, 89 :33–49, 1978.

[4] M. Bryndum, V. B. Jacobsen, and L. Brand. Hydrodynamic forces from wave and current loads on marine pipelines. In *Offshore Technology Conference*, pages –, Houston, Texas, 1983. Offshore Technology Conference.

[5] M. B. Bryndum, V. Jacobsen, and D. T. Tsahlis. Hydrodynamic forces on pipelines : model tests. *Journal of Offshore Mechanics and Arctic Engineering*, 114 :231–241, 1992.

[6] R. Coggan and M. Diesing. The seabed habitats of the central English Channel : A generation on from Holme and Cabioch, how do their interpretations match-up to modern mapping techniques ? *Continental Shelf Research*, 31 :S132–S150, 2011.

[7] Det Norske Veritas (DNV). *Recommended Practice. DNV-RP-C205. Environmental Conditions and Environmental Loads*, 2010. 124 pp.

[8] W. D. Grant and O. S. Madsen. Combined wave and current interaction with a rough bottom. *Journal of Geophysical Research*, 84(C4) :1979–1808, 1979.

[9] M. Kiya. Study on the turbulent shear flow past a circular cylinder. *Bulletin of the Faculty of Engineering, Hokkaido University*, 50 :1–101, 1968.

[10] K. Lambrakos, J. Chao, H. Beckman, and H. Brannon. Wake model of hydrodynamic forces on pipelines. *Ocean Engineering*, 14 :117–136, 1987.

[11] O. S. Madsen. Spectral wave-current bottom boundary layer flows. In *Bottom boundary layer flow*, chapter 29, pages 384–398. Coastal Engineering, 1994.

[12] A. A. Oner, M. Kirkgoz, and M. Akozb. Interaction of a current with a circular cylinder near a rigid bed. *Ocean Engineering*, 2008.

[13] S. R. Sabag, B. L. Edge, and I. R. Soedigdo. Wake II mode for hydrodynamic forces on marine pipelines including waves and currents. *Ocean Engineering*, 27 :1295–1319, 2000.

[14] S. K. Sarkar and S. Sarkar. Vortex dynamics of a cylinder wake in proximity to a wall. *Journal of Fluids and Structures*, 26, 2010.

[15] T. Sarpkaya. Vortex Shedding and Resistance in Harmonic Flow about Smooth and Rough Cylinders at High Reynolds Numbers. Technical Report NPS-59 SL76021, U.S. Naval Post Graduate School, 1976.

[16] H. Schlichting. *Boundary Layer Theory*. McGraw Hill, New York, 1979.

[17] I. R. Soedigdo, K. F. Lambrakos, and B. L. Edge. Prediction of hydrodynamic forces on submarine pipelines using an improved Wake II Model. *Ocean Engineering*, 26 :431–462, 1999.

[18] B. M. Sumer, B. L. Jensen, and J. Fredsøe. Effect of a plane boundary on oscillatory flow around a circular cylinder. *Journal of Fluid Mechanics*, 225 :271–300, 1991.

[19] J. Thiebot, P. B. du Bois, and S. Guillou. Numerical modeling of the effect of tidal stream turbines on the hydrodynamics and the sediment transport e Application to the Alderney Race (Raz Blanchard), France. *Renewable Energy*, 75 :356–365, 2015.

[20] R. Verley, K. Lambrakos, and K. Reed. Prediction of hydrodynamic forces on the seabed pipelines. In *Proc. Offshore Technology Conference*, volume 550, pages 171–180, Houston, 1987. OTC.